Light-induced electrohydrodynamic instability in plasmonically absorbing gold nanofluids

Sujan Shrestha, Jorge Luis Dominguez-Juarez, and Luat T. Vuong

Light-Induced Electrohydrodynamic Instability in Plasmonically Absorbing Gold Nanofluids

Sujan Shrestha[1], Jorge Luis Dominguez-Juarez[2], and Luat T. Vuong[1,3]

Department of Physics, Queens College of the City University of New York, Flushing, NY 11367 USA

Cátedras CONACyT, CFATA, Universidad Nacional Autònoma de México,

Boulevard Juriquilla 3001, Querétaro 76230, México and

Department of Physics, Graduate Center of the City University of New York, New York, NY 10016 USA[*]

(Dated: April 13, 2017)

Plasmonically-absorbing nanofluids exhibit light-induced electrokinetics. We measure an electrical response to the light-induced Rayleigh-Bérnard-Marangoni convective instabilities in gold (Au)-polyvinylpyrrolidone (PVP) nanoparticles (NPs) suspended in isopropanol (IPA) and water. Micro-ampere current oscillations are measured and attributed to the presence of the Au-PVP NPs with negative zeta potential, in correspondence with the accompanying thermal lens oscillations and a nanofluid thermoelectric effect. The measured electrical oscillations represent a new electrohydrodynamic stability driven by light, one among many that should be observed with plasmonic nanoparticles in liquids.

I. INTRODUCTION

First reported in 1965, laser-induced thermal lensing is caused by the change in refractive index that accompanies a temperature gradient from a laser-beam optical axis[1]. At threshold powers, at threshold distances from the free surface or meniscus of a liquid, and in sufficiently absorbing media, the thermal lensing becomes oscillatory. The thermal lens oscillations (TLOs) are often referred to as "optical heartbeats" because the cycles occur at the approximate rate of a Hertz and also exhibit a sharp disruptive jump at the beginning of each cycle. The TLOs are observed when light passes either parallel or perpendicular to the free surface and are first observed in 1982 with an Argon-ion laser in toluene containing cobalt nanoparticles (NPs)[2]. The TLOs represent a light-induced, interacting thermal boundary that itself depends on the dynamics of the system, and consequently, a wide range of complex dynamical behavior is associated with TLOs[2].

The TLOs represent a class of the Rayleigh-Bénard-Marangoni convective instability with a local heating source. As with any Rayleigh-Bénard-Marangoni system, the dynamics of the TLOs are controlled by buoyancy or a Bénard-Rayleigh effect, and surface tension or Bénard-Marangoni effect. Gouesbet *et al.* has extensively studied TLOs in silicon oil with red organol dye[2–5]. According to Gouesbet, the dynamics of the system are controlled by the balance between the convective transfer of heat from the bulk to the surface due to thermal buoyancy and its dissipation due to surface tension disturbances[5]. Gouesbet is able to simulate the dynamics of TLOs by further considering that surface tension dominates when the light is near the surface and conversely, buoyancy dominates when the light absorption is far from the surface[5]. The silicone oil system is the most popular media for the study of free surface instabilities[6], where the thermal buoyancy disrupts surface tension at the oil-air interface. However, systems where the surface tension or Marangoni effect is mediated by the free-surface mass flux are understudied, especially with those containing water[7]; subsequently, TLOs are not widely reported in water[4].

We have demonstrated TLOs in water with plasmonically-absorbing Au nanofluids[8] and also shown that the TLOs depend on the solvent polarity. The characteristics of the TLOs studied here differ from those by Gouesbet in a few, nontrivial ways. Firstly, the TLOs are conducted in water and enhanced by adding an appropriate organic solvent *e.g.* isopropanol (IPA). The water-IPA-air interface is open as opposed to the almost-adiabatic boundary at the free surface of the silicon oil, and therefore the free surface mechanism is different. Finally, since Au nanofluids do not exhibit an appreciable increase in thermal conductivity over its base liquid[9], the TLOs are attributed to the enhanced absorption due to the surface plasmon resonance[10].

Here, we report a new phenomenon of a Rayleigh-Bénard-Marangoni-inspired electrohydrodynamic instability that is present as a consequence of the thermal gradient and surface-tension-driven convective instability and Au-PVP interaction that is directly measured at the surface of the nanofluid. This phenomenon is described by the changes in the Au-PVP NPs fluxes that occur as a result of convective instabilities *i.e.,* temperature gradient and surface tension. The net negative charge on the Au-PVP NPs arises due to Au-PVP interactions[11]. The negative charge can also arise due to localized heating of NPs by laser and accumulation of charged ions on the surface by surface-localized thermodiffusion[12–14].

The negative charge on the nanoparticles allows us to measure the Rayleigh-Bénard-Marangoni instability via electrokinetic behavior that has only recently been explored[15]. The electrohydrodynamic instability described here is different from the conventional electrokinetic instability studied in nanofluidic or microfluidic devices under a strong applied potential field[16]; here, no external electric field is applied and an air/liquid interface exists in the absence of a channel. This research is relevant to the future development of micro or nanofluidic devices, towards the analysis and detection of biological and chemical phenomena on chip, as well as nanoprinting and energy-harvesting phenomena with nanofluids[14,16–18].

II. MATERIALS AND METHODS

The optical set-up in this study is previously described[8]; here we probe the optically-induced electrochemical behavior of the liquid. The voltage and the current between the silver wire (0.05 cm thick) and the silver foil attached to the base are measured, while a collimated (0.9-mm diameter) horizontally-polarized beam ($\lambda = 532nm$) is passed through the cuvette (Fig. 1a). The tip of the wire electrode is within a depth of 1 mm from the surface. The cuvette is filled with a stock solution of polyvinylpyrrolidone (PVP)-coated gold (Au) nanoparticles (0.05 mg/ml, NanoComposix) and isopropanol (99.999%, SigmaAldrich), which are mixed in the ratio of 1 to 2 by volume in a quartz cuvette ($1cm \times 1cm$). The distance between the silver wire and the silver base is kept constant at about 1 cm unless otherwise mentioned and the solution is agitated before every measurement. In our experiments, the silver wire is the electrical ground. The distance between the surface and the laser beam is determined by translating the cuvette vertically in order to achieve a position at which the oscillations are achieved at a specified intensity. Subsequently, the light intensity is reduced so that the far-field thermal-diffraction ring pattern is no longer visible, but light is still
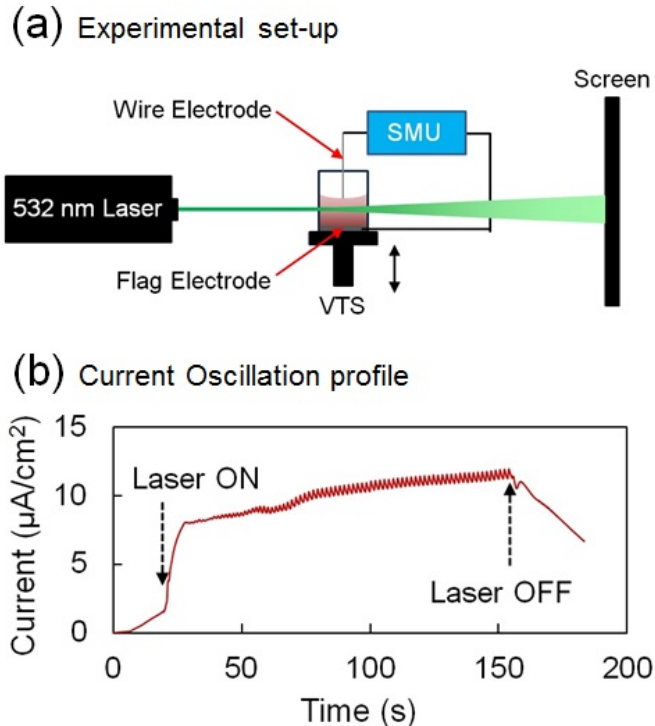
FIG. 1. (a) A side view of the experimental set-up. A horizontally-polarized collimated beam of light of 532-nm wavelength 0.9-mm diameter propagates through a quartz cuvette of 1-cm optical path length, which is filled with a solution containing 80-nm gold nanoparticles (NPs). The vertical motion of the cuvette is controlled with a vertical translation stage (VTS). The electrical current is measured using a source measurement unit (SMU) between a silver wire electrode and a silver flag electrode is fixed to the bottom of the cuvette. (b) A typical current vs. time profile of 80-nm Au NPs in a base fluid composed of water and isopropanol in a ratio of 1 to 2. The laser power is 350 mW and the distance of the laser beam from the surface was ca. 0.6 mm.

transmitted through the sample. The cuvette is lowered so that the edge of the laser grazes the the meniscus, which is indicated by scattering in the far-field beam pattern. When the samples are covered, the COs occur while liquid condenses on the top cover and sides of the cuvette.

Our measurements employ a Keithley Sourcemeter 2636A or source multimeter unit (SMU). The electrochemical behavior of the light-induced TLOs in the Au NP water:IPA mixture is studied by inspection of the electrical current (rather than voltage) response because the SMU exhibits greater current sensitivity. The SMU has a voltage measurement accuracy of $0.015\% + 225\mu$V in the 200 mV range, while the current measurement accuracy is $0.15\% + 120$ fA in the range of 100 pA. The current profiles are recorded with a time resolution of 0.1 s.

Images of the particle flow are taken with a Thorlabs CCD camera from the side of the cuvette in order to observe the colloid behavior. CCD images are captured with XGA sensor resolution (1024 x 768), which provide a full frame repetition rate of 30 fps. Side-view images from the 1-cm glass cuvette with the nanofluid are obtained using the CCD camera with one uncoated bi-convex lens with 100-mm focal length in addition to the Thorlabs C-Mount Camera Lenses (MVL50HS). The image and aperture are adjusted manually. Manual filters reduce the light intensity. The velocity field of NPs is mapped with a Particle Tracking Velocimetry (PTV) open source software. The PTV lab software calculates particle velocity by tracking the centroid of a particle with Integrated Cross-Correlation and Relaxation Method (ICCRM) algorithm developed by Brevis, et al.[19]. We believe that larger clusters of the nanoparticles behave as trackers for the liquid. We also measure the TLOs on a screen in the far field.

III. RESULTS

Fig. 1(b) shows a typical current(I)-time (t) profile where simultaneous TLOs are also obtained. Before the light is turned on, the $I - t$ profile represents a base noise, characteristic of the system set-up. Immediately after the laser is turned on, a steep rise in the current is observed. The steep jump is followed by a transition towards a slow and

steady increase. Then, the current slowly gains oscillations that are invariant over time. If we ignore the oscillations, the average current continues to increase so that the current oscillations (COs) appear as a modulated perturbation to an increasing current profile. In this study, we are interested in the COs, not the average current response. The average current response is defined as a Seebeck effect and is associated with a thermoelectric response[13,14,20–27].

The COs and the TLOs commence simultaneously and their coincident trends confirm that their instabilities are consequences of the same convective instabilities; COs are manifestations of the nanofluid thermoelectric material properties and TLOs are manifestations of thermo-optic behavior. At the same time, it is important to frame the causal, coupled dynamics: TLOs are caused by the fluctuations in the thermal gradients that give rise to oscillatory Fresnel patterns[8] while the COs do not necessarily accompany the TLOs, and simply imply a change in the flux of charged carriers at the surface of the electrodes. In our nanofluid system, the charged carriers are the Au-PVP NPs, which exhibit a negative zeta potential.
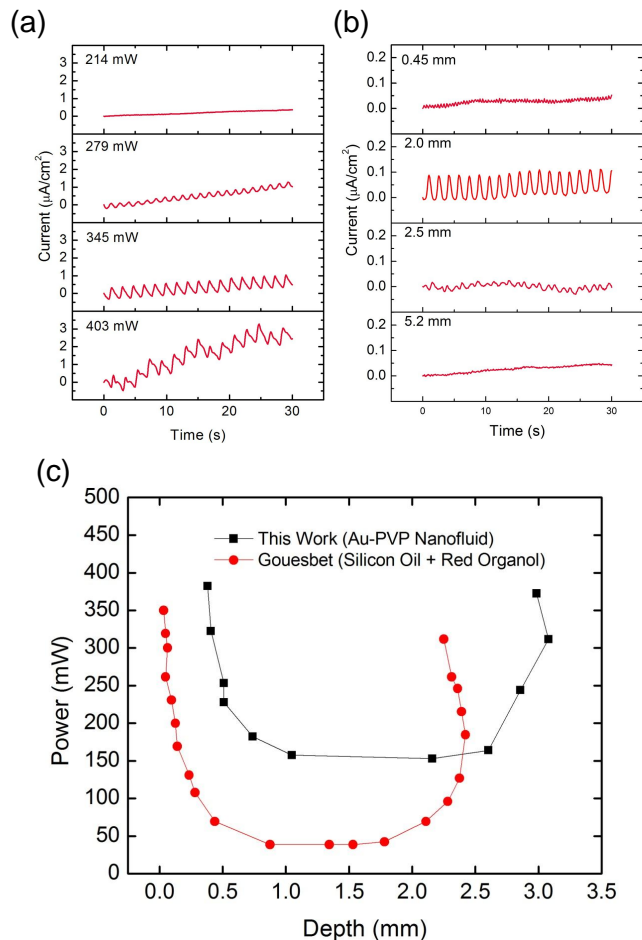

FIG. 2. (a) Plot of the change in the electrical oscillations as a function of the laser beam intensity. The distance of the laser beam to the meniscus is kept constant. (b) The plot of the change in the electrical oscillations as a function of depth. The laser beam intensity is kept constant at 440 mW while oscillations in the measured current and far-field beam profiles are observed. (c) Phase diagram of the primary dynamics of the electrical oscillation in the plane of power and distance of the laser from the free surface for this work and that of Gouesbet[5]. Below the solid line, electrical or optical oscillations are not observed. At most points on this phase diagram above the solid line, the measured currents are nonlinear.

The dynamics of COs and TLOs depend on the laser power and the depth of the laser light from the surface (Fig.2). There is a threshold power at each depth at which the COs commence and a finite range of parameters that sustain the COs. Larger oscillations in the TLOs coincide with larger CO amplitudes. Therefore, the threshold dynamics of COs and TLOs are easily viewed on a stability phase plot with the parameters of power and depth [Fig. 2(c)]; the region above the curve represents the power-depth domain where oscillations occur and the region below the curve represents the power-depth domain where oscillations do not occur. The behavior reflects the power-depth stability phase plot of silicone oil/red organol of Gouesbet, *et. al.*[2]. The shift in the power-depth stability phase plot between

this work and that of Gouesbet, *et. al.* is attributed to the use of different fluids.

There is a complex interplay between evaporation-led surface tension gradients and the thermal gradient produced by the laser due to the presence of the alcohol-aqueous matrix. Previous works in alcohol-water mixtures[28] and other articles concerning tears of wine phenomena) have shown that the evaporation mostly occurs at interface between the mixture and the container wall. The resulting surface tension gradient at the free surface due to evaporative flux couples to the thermal gradient produced by the laser. Moreover, small changes in alcohol-water concentration would significantly increase the surface tension gradient[29], Subsequently, the low-power-threshold COs exhibit hydrodynamic behavior and coupling between thermal gradient and surface tension that is complicated by the alcohol-water binary mixture and the role of thermal heating with the plasmonic nanoparticles, which are known to exhibit a thermophoretic response, in lowering power threshold for producing CO cannot be denied as such COs are not observed in the absence of the nanoparticles in water-alcohol mixtures.
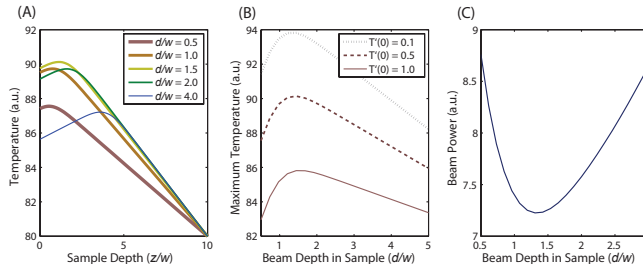

FIG. 3. (A) Numerically-calculated steady-state temperatures as a function of the normalized sample depth $T(z/w)$ where $T'(0) = 0.5$ and w is the width of the Gaussian intensity or absorbed-light energy profile. (B) The maximal temperatures achieved as a function of the normalized input beam depth $T(z/w)$ where the change of the temperature at the free surface $T'(0) = 0.1, 0.5, 1.0$. (C) Input beam power required as a function of normalized input beam depth in order to achieve a fixed threshold temperature when $T'(0) = 0.5$.

A simple evaluation of the heat equation indicates that the highest peak temperatures are achieved in the nanofluid when light enters at an intermediate depth from the free surface, in a manner that agrees with our experimental trends. We evaluate the heat equation in one dimension and incorporate only diffusion and absorption, where the nanofluid is heated by the absorption of a Gaussian light intensity profile that is centered at a depth d from the nanofluid free surface: $\partial^2 T/\partial z^2 = kI$, where k is a constant proportional to the absorption and beam power and inversely proportional to the nanofluid diffusivity, T is the temperature, and the incident beam has a normalized intensity profile $I = \exp[-(\frac{z-d}{w})^2]$. No light is absorbed above the free surface ($z = 0$) and the free surface provides a semi-insulating boundary condition where $dT(0)/dz = \epsilon$. In addition, at a distance $z = 10w$ or the bottom of the nanofluid sample, the temperature is fixed. Evaluation of the heat equation yields a maximum steady-state temperature at a location $z = d$ that is achieved when the beam enters at an intermediate depth of $d \approx 1.5w$ [Fig.3(A)]. This intermediate depth is an optimal balance maximizing absorption over diffusion: when the d is small, diffusion is limited and leads to higher temperatures, but absorption is also reduced since less light penetrates and is absorbed by the nanofluid. The highest steady-state temperatures occur when light enters at an intermediate depth from a free surface $d \approx 1.5w$. Our mathematical analysis indicates that the highest temperatures are achieved at the surface and in the nanofluid when the laser beam enters at a distance of approximately one beam diameter below the surface. This would agree with prior analyses of the thermal cycles with heated wires[2], where it is shown that the temperature gradient is in the horizontal direction, along the meniscus. Our model is narrow in scope and does not account for the surface tension effect or the evaporation effect at the interface; the analysis indicates that there exists a threshold temperature gradient without identifying the underlying effects on the oscillation.

The 1-D evaluation of the steady-state temperatures may also predict other experimental trends of the COs and TLOs. In Fig. 3(B) we vary the boundary diffusion condition ϵ at the free surface and show that the higher steady-state temperatures are achieved when ϵ is smaller. In Fig. 3(B) we also observe that the peak temperature T remains largest when the beam enters the sample at a finite depth $d \approx 1.5w$ even as ϵ changes. In a manner consistent with this analysis: when we experimentally vary the input light power by a factor of 5, the beam depth at which we observe the strongest oscillations remains at approximately 1-1.5 beam widths below the free surface. Better agreement between thermal analyses and experimental trends would be expected if the steady-state convective currents are evaluated in 2-D or 3-D heat equation.

Yet evaluation of the 1-D heat equation indicates that there exists a minimum threshold temperature that is

necessary in order to drive the Rayleigh-Bénard-Marangoni instability. In 3(C) we plot the value of k that scales the steady-state temperature to a fixed constant, in order to estimate the required CO/TLO threshold powers as a function of depth d. The curve provides a power-depth phase plot that may be compared with the experimentally-measured phase plot [Fig.2(c)]; both curves are concave and tilted towards the surface, with a minimum power threshold at an intermediate depth when light enters at 1.5 beam widths from the free surface $d \approx 1.5w$. While the Rayleigh-Bénard-Marangoni instability is widely connected to several power-threshold models invoking analogies to glow discharges or dripping faucets[30,31], the explicit claim of a temperature threshold, especially with respect to the free surface, is not stated. In addition, the physical mechanism underlying a threshold temperature is not yet articulated.
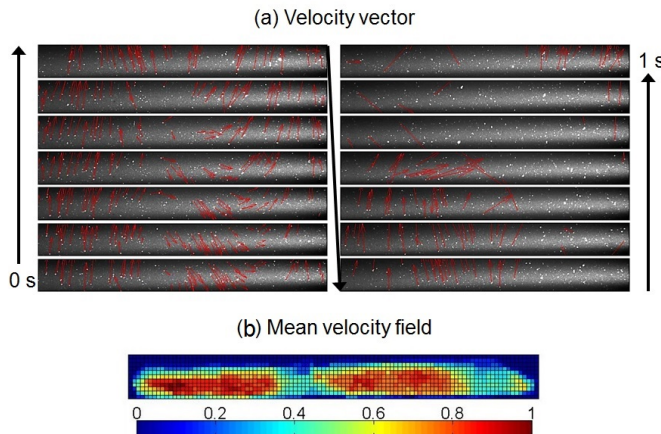

FIG. 4. (a) Images showing the velocity vector flows of 80-nm gold NPs along the path of the laser light (300 mW) at various time frames. These images are taken with a CCD camera from the side of the cuvette: the laser beam enters the cuvette from the right face. The gold NPs are tracked with an open-source particle tracking velocimetry software[19]. (b) Normalized velocity field of gold NP motion. The lower number indicates the regions where the NPs exhibit less motion.

We study the Rayleigh-Bénard-Marangoni instability by directly imaging the fluid motion from the side view. The oscillatory convective pattern is observed as a function of time and also as a function of the horizontal path through the nanofluid (Fig.4(a). The oscillatory motion is explicitly visible in the mean velocity field of the illuminated region (Fig.4(b); the red regions are the areas where the NPs exhibit the most activity or movement. Along the horizontal axis, the particle motion is centered along the optical path of the laser light. The convective oscillatory motion also appears to be axisymmetric around the vertical axis, and as the width of the cuvette increases, this axisymmetric nature of the convection may become smaller. It is not confirmed whether the axisymmetric flow is due to the effect of confinement or due to the evaporation at the interface between the solution and cuvette. Further experiments with wider cuvettes and better understanding of the evaporation may distill the driving force of the hydrodynamic effects in the binary-solvent nanofluid instabilities.
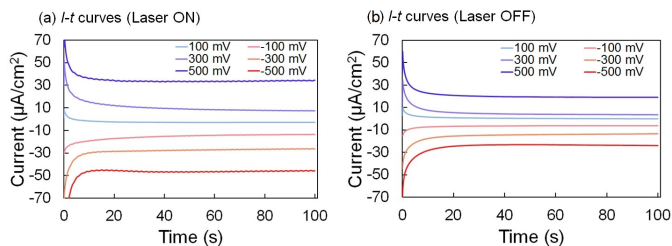

FIG. 5. (a, b) Response of Au-PVP nanofluid to applied bias voltages shown as current (I) vs. time (t) curves in the presence and absence of the laser beam in a two-electrode set-up; the working electrode is a silver wire and the counter/reference electrode is a silver flag. The intensity of the laser is 440 mW and it travels at a depth of 2.2 mm from the free surface. The distance between the electrodes is kept constant.

Our claim that the COs arise from the oscillating convective flux of Au-PVP NPs has important consequences in characterizing the electrochemical behavior of the nanofluid; the dynamic thermal gradients produce transient internal fields and flows that further influence the COs. We measure the transient effects of the applied electrical field on the COs by applying bias voltages from 0.5 V to -0.5 V in the steps of 0.1 V (Figs. 5. The current-time $I - t$ curves

at these voltages show no oscillation in the absence of light, as expected. The current does not tend to zero as time goes to infinity as in the case of pure diffusion limitation or capacitor charge/discharge[32] but acquires a stable value showing a strong ohmic dependence on solution resistance ($V = IR$). In the presence of light, COs are not only evident, but also the average current is greater, which can be attributed to the convection and decrease in resistivity due to thermal heating. Moreover, the COs do not depend on the direction of the applied electric field but on the magnitude of the electric field: in Figs. 4(a,b) we observe that the magnitude of the COs is attenuated as the biased voltages decrease.

IV. DISCUSSION

The electrochemical behavior of the nanofluid, in the absence of the oscillations and in response to the thermal gradient, can be described on the basis of the Seebeck effect. It is known that the temperature gradient induces charge separation resulting in net voltage or electromotive force. The Seebeck effect is attributed to the flow of PVP-coated Au NPs: it is shown that the charge-transfer interaction with the PVP leads to the AuNP acquisition of net negative charge[11]; it is also shown that surface-functionalized Au NPs separate based on size and shape in the presence of electric field in gel electrophoresis[33]; our $I - t$ measurements that show that higher average currents (Figs. 1, 5) are attributed to the Seebeck effect.

The question that we seek to answer is: what is the source of the convective instability in an evaporating system with a free surface and how does it affect the current measurements? We argue that the source of the TLOs and COs are the oscillatory convective instabilities of Au-PVP NPs because we observe a robust oscillatory convective instability of Au-PVP NPs simultaneously with COs (Fig. 4a). The convective instability is influenced by surface tension, as viewed by the axisymmetric flow about the vertical axis that is centered at the optical axis [Fig. 4b]. This flow field manifests in a manner similar to the drying of liquid droplets, which is well-studied and described as a Marangoni effect[34,35]. Figure 4(b) provides the velocity field in the bulk nanofluid close to the light path far from the meniscus. The forward-backward symmetry indicates that the convective instability could be forced by surface tension gradients.

Our nanofluid system with a vertically-axisymmetric flow field and associated Marangoni effect represents an "inverted" drying liquid droplet[35]. In slowly evaporating liquid droplets, the mass flux at the contact line along the edges generates an unequal distribution of the temperature about the surface resulting in a surface tension gradient that is axisymmetric about the vertical central axis[35–38]. With evaporating liquid in a cuvette, the mass flux largely takes place at the three-phase-junction between the solution, air, and cuvette wall. Since IPA has a higher vapor pressure and lower surface tension than that of water, the concentration of water is higher at the three-phase-junction than at the bottom of the meniscus. Hence, a concentration gradient forms and, as a consequence, the surface tension gradient persists with higher surface tension at the contact line of the meniscus than at the bottom of the meniscus. Subsequently, fluid flows from the bottom of the meniscus to the contact line in order to balance the stress that is created by the surface tension gradient.

Since evaporation causes the surface tension gradient to persist, a perpetual convection cell forms near the surface. To conserve mass, fluid from below the bottom of the meniscus flows upwards. The convective flow due to the surface tension gradient acts as a source of the perturbation to convective flow at the bulk as confirmed by Fig. 4. Hennessey and Mnch have simulated the Marangoni instabilities in a slowly evaporating solvent-polymer mixture with a deformable free surface and found that oscillatory instabilities occur more easily in binary-fluid interfaces with a low Marangoni number[39]. This result would agree with our hypothesis and the presence of a TLO temperature threshold, since the surface tension gradients of aqueous-alcohol binary-fluids are more sensitive to changes in temperature[40].

The oscillatory convective instability affects the current because the flux of the charged Au-PVP NPs at the electrode surface is also dependent on the convection. The convection determines the concentration of the species at the boundary of the diffusion layer in the diffusive-convective model or Debye length, the effective length of screening layer made up of oppositely-charged ions in the diffuse double-layer model[32]. Therefore, the oscillatory convective instability will fundamentally perturb any current measurements (5). Interestingly, the COs show dependence on the magnitude of the applied voltages (Fig. 5), which affect the migration of the charged particles. When the silver wire is positively biased, the electromigration of the negatively-charged Au-PVP NPs towards the electrode increases. Conversely, when the silver wire is negatively biased, the electromigration of the negatively charged Au-PVP NPs away from the electrode increases. In both cases, the oscillatory convection near the surface is reinforced. Hence, the change in direction of the electric field at this small magnitude did not change the COs. This shows that the COs can be enhanced with the application of an external electric field.

It is well understood that the Rayleigh-Bernard instability is attributed to a thermal gradient, while convection is attributed to a density gradient i.e. fluid rising due to buoyancy, and that both effects are present in the Rayleigh-Bernard-Marangoni instability via surface tension effects. The presence of nanoparticle surface charge is not entirely

yet clear, however the combination of nanoparticle thermophoresis influences the flow and convection, resulting in electrohydrodynamics. There are aspects of the Rayleigh-Bénard-Marangoni-type instabilities that are not yet well understood for colloidal systems largely related to the thermal-convective flows[41], and such thermal-convective flows are more complex in plasmonic nanofluids. Specifically, the thermophoretic mechanism is outlined at the microscopic level[42], but the nanoparticle thermophoresis depends strongly on the particle-solvent interface rather than bulk or surface properties[42–44]. To the best of our knowledge, the only paper to measure the thermophoretic Soret coefficient of a plasmonic nanoparticle is Gargiulo *et al.*[18]. Although it is measured to be repulsive, where particles flow from cold to hot, we image plasmonic clusters traveling in reverse, from cold to hot. Knowledge of the plasmonic nanoparticle thermophoresis may enable proper optimization of electrokinetic instabilities and thermoelectric behavior.

V. CONCLUSIONS

In summary, we demonstrate a new electrohydrodynamic instability in plasmonic nanofluids that represent a sub-family of light-induced Rayleigh-Bénard-Marangoni instabilities. The oscillations are due to the ionic current associated with Au-PVP NPs, which have a net zeta potential. The electrical oscillations are a measure of the convective instabilities of the Au-PVP nanofluid due to Marangoni effect established by evaporation at the contact edges mirroring the drying droplet and "tears of wine". Hence, the electrical oscillations reveal the dynamics of the system. We show that the threshold for observing the oscillations is correlated with the maximum steady-state temperature that is achieved and hypothesize that there exists a temperature threshold for observing the TLOs. The characteristics of the self-synchronizing electrohydrodynamic instability vary with voltage bias, surface tension, incident power, and depth. Our knowledge of the oscillations is relevant to the understanding of photoelectrochemical and thermochemical responses where there is a free interface.

VI. ACKNOWLEDGMENT

---

[*] Corresponding author: luat.vuong@qc.cuny.edu

[1] J. P. Gordon, R. C. C. Leite, R. S. Moore, S. P. S. Porto, and J. R. Whinnery, "Long-transient effects in lasers with inserted liquid samples," Journal of Applied Physics **36**, 3–8 (1965).

[2] G. Gouesbet, C. Roze, and S. Meunier-Guttin-Cluzel, "Instabilities by local heating below an interface," Journal of Non-Equilibrium Thermodynamics **25**, 337–379 (2001).

[3] G. Gouesbet and E. Lefort, "Thermal lens oscillations at low laser power," Applied Optics **26**, 2940–2941 (1987).

[4] G. Gouesbet and E. Lefort, "Dynamical states and bifurcations of a thermal lens using spectral analysis," Physical Review A **37**, 4903–4915 (1988).

[5] G. Gouesbet, "Simple model for bifurcations ranging up to chaos in thermal lens oscillation and associated phenomena," Physical Review A **42**, 5928–5945 (1990).

[6] Michael F Schatz and G Paul Neitzel, "Experiments on thermocapillary instabilities," Annual Review of Fluid Mechanics **33**, 93–127 (2001), http://dx.doi.org/10.1146/annurev.fluid.33.1.93.

[7] Khellil Sefiane and Charles A. Ward, "Recent advances on thermocapillary flows and interfacial conditions during the evaporation of liquids," Advances in Colloid and Interface Science **134135**, 201 – 223 (2007).

[8] J. L. Dominguez-Juarez, S. Vallone, A. Lempel, M. Moocarme, J. Oh, H. D. Gafney, and L. T. Vuong, "Influence of solvent polarity on light-induced thermal cycles in plasmonic nanofluids," Optica **2**, 447–453 (2015).

[9] Natallia Shalkevich, Werner Escher, Thomas Brgi, Bruno Michel, Lynda Si-Ahmed, and Dimos Poulikakos, "On the thermal conductivity of gold nanoparticle colloids," Langmuir **26**, 663–670 (2010), http://dx.doi.org/10.1021/la9022757.

[10] Alexander O. Govorov and Hugh H. Richardson, "Generating heat with metal nanoparticles," Nano Today **2**, 30 – 38 (2007).

[11] Manoranjan Behera and Shanker Ram, "Spectroscopy-based study on the interaction between gold nanoparticle and poly(vinylpyrrolidone) molecules in a non-hydrocolloid," International Nano Letters **3**, 1–7 (2013).

[12] Y Takeuchi, T Ida, and K Kimura, "Colloidal stability of gold nanoparticles in 2-propanol under laser irradiation," Journal of Physical Chemistry B **101**, 1322–1327 (1997).

[13] Arghya Majee and Alois Würger, "Collective thermoelectrophoresis of charged colloids," Physical Review E **83**, 061403 (2011).

[14] Arghya Majee and Alois Würger, "Charging of heated colloidal particles using the electrolyte seebeck effect," Physical Review Letters **108**, 118301 (2012).

[15] Touvia Miloh, "Opto-electro-fluidics and tip coax conical surface plasmons," PHYSICAL REVIEW FLUIDS **1** (2016), 10.1103/PhysRevFluids.1.044105.

[16] Hao Lin, "Electrokinetic instability in microchannel flows: A review," Mechanics Research Communications **36**, 33 – 38 (2009), recent Advances in Microfluidics.

[17] Shizhi Qian, Sang W. Joo, Yingtao Jiang, and Marcos A. Cheney, "Free-surface problems in electrokinetic micro- and nanofluidics," Mechanics Research Communications **36**, 82 – 91 (2009).

[18] Julin Gargiulo, Santiago Cerrota, Emiliano Corts, Ianina L. Violi, and Fernando D. Stefani, "Connecting metallic nanoparticles by optical printing," Nano Letters **16**, 1224–1229 (2016), pMID: 26745330, http://dx.doi.org/10.1021/acs.nanolett.5b04542.

[19] W. Brevis, Y. Niño, and G. H. Jirka, "Integrating cross-correlation and relaxation algorithms for particle tracking velocimetry," Experiments in Fluids **50**, 135–147 (2011).

[20] George Guthrie, J. Norton Wilson, and Verner Schomaker, "Theory of the thermal diffusion of electrolytes in a clusius column," The Journal of Chemical Physics **17**, 310–313 (1949).

[21] J. N. Agar and J. C. R. Turner, "Thermal diffusion in solutions of electrolytes," Proceedings of the Royal Society of London A: Mathematical, Physical and Engineering Sciences **255**, 307–330 (1960), http://rspa.royalsocietypublishing.org/content/255/1282/307.full.pdf.

[22] Hubert H. Girault, "The water/oil/water thermocouple and the ionic seebeck effect," Journal of the Chemical Society , Faraday Transactions 1 **84**, 2147–2154 (1988).

[23] J. N. Agar, C. Y. Mou, and Jeong Long Lin, "Single-ion heat of transport in electrolyte solutions: a hydrodynamic theory," The Journal of Physical Chemistry **93**, 2079–2082 (1989), http://dx.doi.org/10.1021/j100342a073.

[24] Alois Würger, "Transport in charged colloids driven by thermoelectricity," Physical Review Letters **101**, 108302 (2008).

[25] Alois Wrger, "Thermal non-equilibrium transport in colloids," Reports on Progress in Physics **73**, 126601 (2010).

[26] Theodore J. Abraham, Douglas R. MacFarlane, and Jennifer M. Pringle, "Seebeck coefficients in ionic liquids -prospects for thermo-electrochemical cells," Chemical Communications **47**, 6260–6262 (2011).

[27] M. Bonetti, S. Nakamae, M. Roger, and P. Guenoun, "Huge seebeck coefficients in nonaqueous electrolytes," The Journal of Chemical Physics **134**, 114513 (2011).

[28] Khellil Sefiane, Samuel David, and Martin E. R. Shanahan, "Wetting and evaporation of binary mixture drops," The Journal of Physical Chemistry B **112**, 11317–11323 (2008), pMID: 18707163, http://dx.doi.org/10.1021/jp8030418.

[29] G Vazquez, E Alvarez, and JM Navaza, "Surface-tension of alcohol plus water from 20-degrees-c to 50-degrees-c," Journal of Chemical and Engineering Data **40**, 611–614 (1995).

[30] Takeshi Hayashi, "Mixed-mode oscillations and chaos in a glow discharge," Physical Review Letters **84**, 3334–3337 (2000).

[31] Piotr Garstecki, Michael J. Fuerstman, and George M. Whitesides, "Nonlinear dynamics of a flow-focusing bubble generator: An inverted dripping faucet," Physical Review Letters **94**, 234502 (2005).

[32] Allen J. Bard and Larry R. Faulkner, *Electrochemical Methods: Fundamentals and Applications*, 2nd ed. (John Wiley & Sons, Inc., 2001).

[33] Xiaoyou Xu, K. Kenneth Caswell, Elizabeth Tucker, Saswat Kabisatpathy, K. Lisa Brodhacker, and Walter A. Scrivens, "Size and shape separation of gold nanoparticles with preparative gel electrophoresis," Journal of Chromatography A **1167**, 35 – 41 (2007).

[34] Rajneesh Bhardwaj, Xiaohua Fang, and Daniel Attinger, "Pattern formation during the evaporation of a colloidal nanoliter drop: a numerical and experimental study," New Journal of Physics **11**, 075020 (2009).

[35] Hua Hu and Ronald G. Larson, "Marangoni effect reverses coffee-ring depositions," The Journal of Physical Chemistry B **110**, 7090–7094 (2006), http://dx.doi.org/10.1021/jp0609232.

[36] Robert D. Deegan, Olgica Bakajin, Todd F. Dupont, Greb Huber, Sidney R. Nagel, and Thomas Witten, "Capillary flow as the cause of ring stains from dried liquid drops," Nature **389**, 827–829 (1997).

[37] Hua Hu and Ronald G. Larson, "Analysis of the effects of marangoni stresses on the microflow in an evaporating sessile droplet," Langmuir **21**, 3972–3980 (2005), http://dx.doi.org/10.1021/la0475270.

[38] Hua Hu and Ronald G. Larson, "Analysis of the microfluid flow in an evaporating sessile droplet," Langmuir **21**, 3963–3971 (2005), http://dx.doi.org/10.1021/la047528s.

[39] Matthew G. Hennessy and Andreas Mnch, "Dynamics of a slowly evaporating solventpolymer mixture with a deformable upper surface," IMA Journal of Applied Mathematics **79**, 681–720 (2014).

[40] Gonzalo Vazquez, Estrella Alvarez, and Jose M. Navaza, "Surface tension of alcohol water + water from 20 to 50 .degree.c," Journal of Chemical & Engineering Data **40**, 611–614 (1995), http://dx.doi.org/10.1021/je00019a016.

[41] A. Ya. Malkin, "Surface instabilities," Colloid Journal **70**, 673–689 (2008).

[42] R Piazza and A Parola, "Thermophoresis in colloidal suspensions," Journal of Physics: Condensed Matter **20**, 153102 (2008).

[43] Alois Würger, "Transport in charged colloids driven by thermoelectricity," Physical Review Letters **101**, 108302 (2008).

[44] Alois Würger, "Hydrodynamic boundary effects on thermophoresis of confined colloids," Phys. Rev. Lett. **116**, 138302 (2016).